NJC

PAPER

View Article Online
View Journal | View Issue

Cite this: *New J. Chem.*, 2014, **38**, 3050

LC-MS/MS characterization of forced degradation products of ambrisentan: development and validation of a stability-indicating RP-HPLC method

Nageswara Rao Ramisetti* and Ramakrishna Kuntamukkala

Received (in Montpellier, France) 16th January 2014,
Accepted 12th March 2014

DOI: 10.1039/c4nj00075g

www.rsc.org/njc

The current study reports the characterization of degradation products of ambrisentan by liquid chromatography-tandem mass spectrometry, and development and validation of a stability-indicating reversed phase high performance liquid chromatographic method for determination of ambrisentan in the presence of its process related impurities in bulk drugs. The drug was subjected to various stress conditions such as hydrolysis, oxidation, photo- and thermal degradations to investigate the stability-indicating ability of the method. Significant degradation was observed during acidic and oxidative stresses. Ambrisentan was well resolved from its process related impurities and degradation products formed under stress conditions. The chromatographic separation was accomplished on an Agilent XDB C_{18} column (150 × 4.6 mm; 5 μm) with the mobile phase consisting of 10 mM NH_4OAc (pH = 5.2) and CH_3CN in a gradient elution mode at a flow rate of 1.0 ml min^{-1}. The eluents were monitored by a photodiode array detector at 215 nm and quantitation limits were obtained in the range of 0.07–0.25 μg ml^{-1} for ambrisentan and all its process related impurities. The developed liquid chromatographic method was validated with respect to accuracy, precision, linearity, robustness and limits of detection and quantitation. The degradation products were characterized by comparing their collision induced dissociation mass spectral data with that of ambrisentan and the most possible degradation and fragmentation pathways were proposed.

Introduction

Ambrisentan (AMB), (+)-(2*S*)-2-[(4,6-dimethylpyrimidin-2-yl)-oxy]-3-methoxy-3,3-diphenylpropanoic acid, is an orally active nonsulfonamide class endothelin receptor antagonist selective for type-A endothelin. It is used in the treatment of pulmonary arterial hypertension (PAH), a rare life-threatening disease characterized by its progressive increase in pulmonary vascular resistance due to elevations in pulmonary arterial pressure causing right ventricular failure and leading finally to death.[1–4] It was approved worldwide under brand names Letairis (US), Volibris (EU), and Pulmonext (India) in various strengths ranging from 2.5–10 mg. There is a strong demand for the characterization of potential impurities (process related impurities and degradation products (DPs)) in the quality control of AMB active substances, not only to ensure safety of its formulations but also regulatory compliance.

A thorough literature survey has revealed that only a few LC methods are available for analysis of AMB. LC-MS was used for determination of AMB in rat plasma.[5] Normal and reversed phase HPLC were also used for separation of AMB enantiomers in the absence and presence of impurities.[6,7] Quite recently, Satheeshkumar and Naveenkumar have reported a stability-indicating RP-HPLC method for determination of AMB assay,[8] but it failed to establish the stability-indicating ability of the method in the presence of all possible process related impurities. Narayana *et al.* have also reported a RP-HPLC method for determination of AMB assay in the presence of a limited number of process related impurities using a mobile phase comprised of non-volatile phosphate buffer which is incompatible for LC-ESI-MS characterization.[9] However, these methods did not address the characterization of stress DPs by mass spectrometry. Thus, there is a great potential for development of analytical methods to monitor the levels of all possible impurities in the bulk drugs of AMB during process development and characterization of DPs to ensure its safety in formulations. In the present study, four process related impurities: methyl 3,3-diphenyloxirane-2-carboxylate (Imp-2), methyl 2-hydroxy-3-methoxy-3,3-diphenylpropanoate (Imp-3), (*S*)-2-hydroxy-3-methoxy-3,3-diphenylpropanoic acid (Imp-4), and 4,6-dimethyl-2-(methylsulfonyl)pyrimidine (Imp-5), were prepared from benzophenone (Imp-1) as described in Scheme 1,[10,11]

HPLC Group, Analytical Chemistry Division, IICT, Tarnaka, Hyderabad-500007, India. E-mail: rnrao55@yahoo.com, rnrao@iict.res.in; Fax: +91 40 27160387; Tel: +91 40 27193193

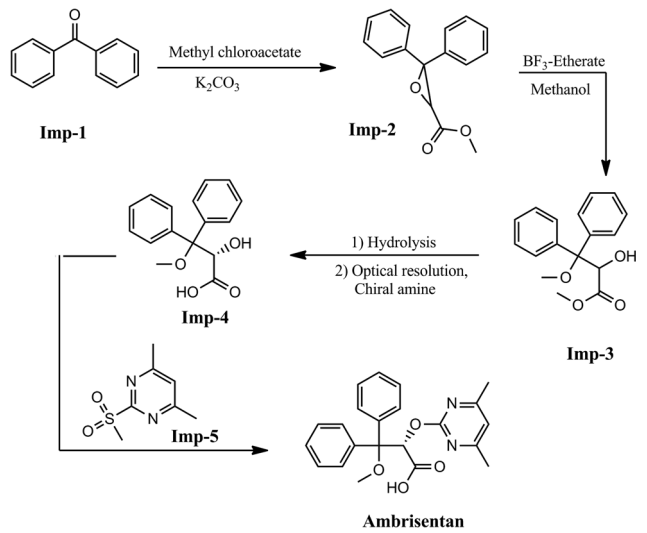

Scheme 1 A schematic representation of the synthesis of ambrisentan.

a validated stability-indicating RP-HPLC method for the determination of AMB and its all five process related substances was developed, and five of its DPs formed under acidic and oxidative stress were characterized by LC-ESI-MS/MS and accurate mass measurements.

Experimental

Chemicals

High purity H_2O was obtained by using a Millipore Milli-Q water purification system (Millipore synergy, France). HPLC grade CH_3CN was purchased from Sigma Aldrich Chemicals Pvt. Ltd, Bangalore, India. Benzophenone (minimum assay 99%), and AR grade NH_4OAc, AcOH, HCl, and NaOH were purchased from SD Fine Chemicals Pvt. Ltd, Mumbai, India. H_2O_2 (27% w/w) from Acros Organics was used for oxidative degradation. A mixture of CH_3CN and H_2O (50 : 50 v/v) was used as diluent. AMB (potency 99.8%) was received as a gift sample from Matrix Laboratories, Hyderabad, India. Related impurities of AMB were synthesized in our laboratory. ^1H NMR ($CDCl_3$, BRUKER AVANCE 300) and HPLC area percentage purity data of synthesized impurities are given below.

Imp-2. δ 3.52 (s, 3H), 3.99 (s, 1H), 7.28–7.46 (m, 10H); HPLC purity 99.2%.

Imp-3. δ 2.96 (d, J = 8.7, 1H), 3.15 (s, 3H), 3.62 (s, 3H), 5.17 (d, J = 8.7, 1H), 7.29–7.44 (m, 10H); HPLC purity 99.8%.

Imp-4. δ 3.17 (s, 3H), 3.41 (br, 1H), 5.08 (s, 1H), 7.29–7.50 (m, 10H); HPLC purity 99.7%.

Imp-5. δ 2.51 (s, 6H), 3.55 (s, 3H), 7.00 (s, 1H); HPLC purity 98.8%.

Instrumentation

High performance liquid chromatography. A prominence series HPLC system equipped with a quaternary UFLC LC-20AD pump, a DGU-$20A_5$ degasser, a SIL-20AC auto sampler, a CTO-20AC column oven, an SPD-M20A diode array detector, and a CBM-20A communications bus module was used for method development, validation and stress degradation studies (all from Shimadzu, Kyoto, Japan.). The chromatographic system was controlled by LC Solution data acquisition software. The chromatographic column used was XDB C_{18} (150 × 4.6 mm, 5 μm) from Agilent. The mobile phase components are (A) 10 mM NH_4OAc (pH adjusted to 5.2 by using 10% AcOH solution), and (B) CH_3CN. The separation was accomplished in a gradient elution program (time (min)/% B: 0.01/27, 12/27, 17/55, 33/55, 34/27, 45/27) at a flow rate of 1.0 ml min^{-1} and at a column temperature of 25 °C. The chromatographic eluents were monitored at a detection wavelength of 215 nm using a photodiode array (PDA) detector. The sample injection volume was 20 μl.

Mass spectrometry. An Agilent 1200 series HPLC instrument coupled to a quadrupole time-of flight (Q-TOF) mass spectrometer (Q-TOF LC/MS 6510 series classic G6510A, Agilent Technologies, USA) equipped with an ESI source was used for identification and characterization of degradation products of AMB. The data acquisition and processing were under the control of Mass Hunter workstation software. In order to allow the entry of only 40% of the chromatographic eluent a splitter was placed before the ESI source. The typical operating source conditions for MS scan in positive ESI mode were optimized as follows: the fragmentor voltage was 80 V; the capillary voltage was 3000–3500 V; the skimmer voltage 60 V. Nitrogen gas was used for nebulization (45 psi) and drying (300 °C, 9 L h^{-1}). For collision-induced dissociation (CID) experiments, keeping MS^1 static, the precursor ion of interest was selected using the quadrupole analyzer and the product ions were analyzed using a time-of-flight (TOF) analyzer. Ultra-high purity nitrogen was used as collision gas at 18 Torr. All the spectra were recorded under identical experimental conditions, and are averages of 20–30 scans.

Preparation of analytical solutions

Stock solutions of AMB (2.0 mg ml^{-1}) and all process related impurities (0.5 mg ml^{-1} each) were prepared separately by dissolving the appropriate amounts in the minimum amount of CH_3CN and diluted to volume with diluent. A stock solution of impurity mixture (0.05 mg ml^{-1} each) was also prepared by mixing impurity stock solutions and made to volume with diluent. Working solutions were prepared by adequately mixing the stock solutions for method development and validation studies.

Specificity and forced degradation

Specificity is the ability of the method to measure the analyte (AMB) response unequivocally in the presence of its possible impurities. The specificity of the developed LC method for AMB was determined in the presence of its process related impurities (Imp-1 to Imp-5 at 0.15%) and DPs. Forced degradation studies can help to identify the likely DPs, also they in turn can help to establish the degradation pathways and the intrinsic stability of the molecule.[12] AMB (1 mg ml^{-1}) was subjected to stress conditions such as acidic (0.5 N HCl, 60 °C, 3 h), basic (0.5 N NaOH, 60 °C, 8 h) and neutral (H_2O, 60 °C, 8 h)

hydrolyses, and oxidation (10% H_2O_2, 24 h) in solution state. AMB was also subjected to thermolytic (60 °C, 10 days) and photolytic (UV light 254 nm, 10 days) stress in solid state. Different stress conditions were followed to achieve significant degradation. Acid and base hydrolyzed samples were neutralized, and all the degradation samples were diluted five times for assay determination. AMB assays were performed by comparison with standard and the mass balances (%assay + %impurities + %DPs) were calculated for stressed samples. The degradation samples were injected into an LC-PDA system to check the purity and homogeneity of the AMB peak. LC-MS was used for the characterization of the DPs.

Method validation

The validation of the HPLC method was carried out for the determination of related substances (*i.e.*, Imp-1 to Imp-5) and assay of AMB as per ICH guidelines to demonstrate that the method is appropriate for its intended use.[13]

System suitability. The system suitability tests were conducted throughout the validation studies by injecting 600 μg ml^{-1} of AMB solution containing 0.9 μg ml^{-1} (0.15%) of all related substances and 100 μg ml^{-1} of AMB solution for related substance and assay methods, respectively.

Precision. The system precisions were checked by analyzing six replicates of standard solutions for both assay (AMB 100 μg ml^{-1}) and related substance (AMB 600 μg ml^{-1} spiked with 0.15% of each impurity) methods individually. The method precisions for assay and related substances were evaluated by injecting six individual test preparations of AMB (100 μg ml^{-1}), and AMB (600 μg ml^{-1}) spiked with 0.15% of each impurity, respectively. The intermediate precision were evaluated with same concentration solutions used for methods precision prepared separately on a different day by different analysts using different instruments located within the same laboratory. Precision at LOQ levels was also determined by injecting six individual preparations of mixtures of all impurities spiked into AMB (600 μg ml^{-1}) at their LOQ level. The %RSDs of the areas of each impurity and AMB were calculated for precision studies.

Limits of detection (LOD) and quantitation (LOQ). The LOD and LOQ values for AMB and related substances (Imp-1 to Imp-5) were determined at signal-to-noise ratios of 3 : 1 and 10 : 1, respectively, by injecting a series of dilute solutions with known concentrations.

Accuracy. Accuracy of the related substance method was evaluated by spiking known amounts of the impurities into the test sample, analyzing the same and calculating the percent recovered. For related substances, the recovery studies were performed in triplicate at four concentration levels (LOQ, 50, 100 and 150%) to specification level (0.15%) of impurities (*i.e.*, LOQ, 0.45, 0.9, and 1.35 μg ml^{-1}) with respect to AMB drug substance concentration 600 μg ml^{-1}. The accuracy of the AMB assay was evaluated in triplicate at the three concentration levels 50, 100 and 150% (*i.e.*, 50, 100 and 150 μg ml^{-1}) to AMB concentration 100 μg ml^{-1}, and the recovery was calculated for each concentration.

Linearity. Linearity of the related substance method was established by analyzing series of dilute solutions at six different concentration levels ranging from LOQ to 250% to the specification level of impurities (*i.e.*, LOQ, 0.45, 0.9, 1.35, 1.8, and 2.25 μg ml^{-1}) spiked into AMB drug substance (600 μg ml^{-1}). The calibration curves were drawn by plotting the peak areas of impurities against their corresponding concentrations. Similarly, assay method linearity was established by injecting AMB at five different concentration levels ranging from 50 to 150% (*i.e.*, 50, 75, 100, 125, and 150%) to AMB concentration 100 μg ml^{-1}. The correlation coefficients (r^2), slopes and *Y*-intercepts of impurities and AMB were determined from their respective calibration plots.

Robustness. The robustness study was carried out to evaluate the influence of small variations in the optimized chromatographic conditions. The factors chosen for this study were temperature of the column (±2 °C), mobile phase pH (±0.2) and flow rate (±0.1 ml min^{-1}). System suitability parameters, and changes in assay of AMB and recoveries of impurities were checked. In all the above deliberately altered experimental conditions, the components of the mobile phases were held constant.

Results and discussion

Method development and optimization of chromatographic conditions

Preliminary experiments were carried out to develop a chromatographic system not only capable of eluting and resolving AMB from its process related impurities and stress DPs but also compatible with LC-MS characterization. In the initial stages of method development, C_{18} columns (Phenomenex Luna and Agilent Extend (250 × 4.6 mm, 5 μm)) were tried. A desirable resolution (>2) between AMB and impurities was achieved with several mobile phase compositions in isocratic elution modes with NH_4OAc/$HCOONH_4$ buffers and CH_3CN/CH_3OH. But AMB peak asymmetry was found to be high (A_s > 1.5) in CH_3OH when compared to CH_3CN. At lower organic mobile phase content, higher retention times of non-polar impurities (Imp-1, Imp-2, and Imp-3), and DP-6 were observed; whereas co-elution of polar impurities (Imp-4, and Imp-5) and DP-3 was observed at higher organic content. A very good separation between all impurities and AMB was accomplished with 20 mM NH_4OAc (pH = 4.2) and CH_3CN in 50 : 50 (v/v) ratio on the Luna-C18 column, but with lack of desirable resolution between polar components Imp-4 and DP-3. Replacement of the C_{18} column with a C_8 column also showed no improved results. To decrease HPLC method run time and good resolutions between all impurities, DPs, and AMB the elution mode was shifted to gradient. In the gradient elution program, the method was initiated with lesser organic content to achieve resolution between polar analytes; and later increased to achieve decreased retention times of non-polar analytes. Under these conditions (20 mM NH_4OAc–$HCOONH_4$, CH_3CN), large base line drift to the negative side (>250 mAU) was observed with different pH (4.0–6.5) buffer combinations. Employing a 15 cm column instead of a 25 cm column was found useful in decreasing the negative base line drift without disturbing the peak parameters to a significant extent by decreasing the variation

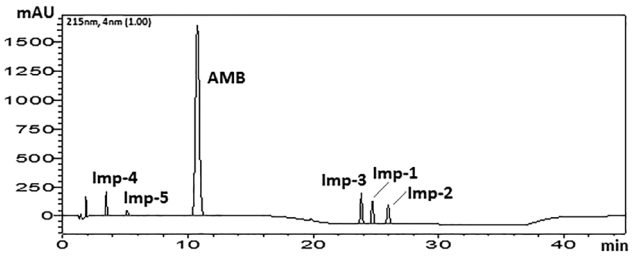

Fig. 1 Chromatogram of AMB (600 μg ml^{-1}) spiked with 1% of all process impurities under optimized chromatographic conditions.

in mobile phase composition from initial to later conditions in the gradient program. The detector wavelength was optimized at 215 nm instead of 225 and 262 nm as mentioned in earlier reports,[8,9] as sensitivity of all the analytes was found to be higher and with visibility of DP-2 and DP-3. Finally, after several attempts, optimized chromatographic conditions were identified as described in the experimental section. The chromatographic separation of AMB (600 μg ml^{-1}) and impurities (6 μg ml^{-1}) under optimized conditions is shown in Fig. 1.

Method validation

System suitability data indicating that the system was suitable for use as the tailing factor for all the analytes was less than 1.5 and the resolution between any of the two adjacently eluting analytes was greater than 2.5. It also confirms the good selectivity of the method. LOD and LOQ results of AMB and its related substances were obtained in the ranges of 0.025–0.08 μg ml^{-1} and 0.07–0.25 μg ml^{-1}, respectively, indicating the higher sensitivity of the method. The %RSD values of peak areas obtained were below 3.7 and 0.8 for related substances and AMB, respectively, indicating good precision of the method. The percentage recoveries of related substances ranged from 93.74 to 105.74 and

Table 1 Validation data

Parameter	Imp-4	Imp-5	AMB	Imp-3	Imp-1	Imp-2
System suitability[a]						
t_R (min)	3.48	5.11	10.55	23.83	24.69	25.95
RRT	0.330	0.484	1.000	2.259	2.340	2.460
RRF	0.84	0.26	1.00	1.12	1.02	0.98
R_s	—	5.91	11.94	29.02	2.53	3.42
k^1	—	0.47	2.03	5.84	6.09	6.45
A_s	1.43	1.20	1.08	1.12	1.06	1.21
N	3252	4490	4834	95 243	72 124	78 311
Linearity						
Range (μg ml^{-1})	0.09–2.25	0.25–2.25	50–150	0.07–2.25	0.1–2.25	0.1–2.25
r^2	0.9999	0.9987	1	0.9984	0.9985	0.9992
Slope	46 179	13 467	66 199	57 828	52 904	54 277
Intercept	−56.43	341.8	−91 467	2010	1009	942.6
Detection limit (μg ml^{-1})	0.03	0.08	0.033	0.025	0.033	0.033
Quantitation limit (μg ml^{-1})	0.09	0.25	0.1	0.07	0.1	0.1
RRF	0.84	0.26	1.00	1.12	1.02	0.98
Precision (%RSD)[a]						
System	0.804	0.418	0.358	1.588	1.514	1.239
Method	1.041	2.133	0.483	0.705	0.445	0.987
Intermediate	3.612	0.766	0.797	2.076	0.997	1.691
LOQ	2.497	2.233	—	1.572	1.363	1.986
Accuracy at 50% level[b]						
Amount added (μg ml^{-1})	0.45	0.45	50	0.45	0.45	0.45
Amount recovered (μg ml^{-1})	0.461	0.442	49.59	0.456	0.457	0.445
%Recovery	102.51	98.21	99.19	101.32	101.59	98.86
Accuracy at 100% level[b]						
Amount added (μg ml^{-1})	0.90	0.90	100	0.90	0.90	0.90
Amount recovered (μg ml^{-1})	0.893	0.903	100.23	0.904	0.878	0.887
%Recovery	99.24	100.35	100.23	100.42	97.59	98.6
Accuracy at 150% level[b]						
Amount added (μg ml^{-1})	1.35	1.35	150	1.35	1.35	1.35
Amount recovered (μg ml^{-1})	1.327	1.327	151.06	1.33	1.379	1.325
%Recovery	99.27	98.31	100.71	98.51	102.14	98.12
Accuracy at LOQ level[b]						
Amount added (μg ml^{-1})	0.09	0.25	—	0.07	0.1	0.1
Amount recovered (μg ml^{-1})	0.092	0.24	—	0.066	0.106	0.095
%Recovery	102.09	95.84	—	93.74	105.74	95.26

t_R, retention time; RRT, relative retention time; R_s, resolution; k^1, retention factor; A_s, tailing factor; N, number of theoretical plates; r^2, correlation coefficient; RRF, relative response factor. [a] Average of six determinations. [b] Average of three determinations.

AMB from 99.19 to 100.71 determining the accuracy of the method. Linearity results of AMB and related substances showed the existence of an excellent correlation ($r^2 > 0.998$) between the peak area and the concentrations. In all deliberately altered chromatographic conditions (flow rate, pH and column temperature), all analytes were adequately resolved and elution order remains unchanged. The resolutions between any two adjacent analytes were obtained greater than 2.0 and tailing factors of all analytes were obtained less than 1.6. The variability in the estimation of AMB assay and related substances was within ±2 and ±9%, respectively, indicating the robustness of the method. The results of system suitability, LOD, LOQ, precision, accuracy and linearity are summarized in Table 1.

Specificity and degradation behavior of AMB

The assay of AMB for three determinations was found to be 99.62% with %RSD 0.16, while in the presence of impurities (0.15% w/w) it was 99.69% with %RSD 0.39. No considerable degradation of AMB drug substance was observed under neutral and basic hydrolytic, photolytic and thermolytic stress conditions. Significant degradation of AMB drug substance was observed in acidic hydrolysis, and oxidation (Fig. 2). Peak purity test results obtained from the PDA detector confirmed that the AMB peak was pure and homogeneous in all the analyzed stress samples. The mass balance of stressed samples was found in the range of 99.3–99.8%. The forced degradation results are summarized in Table 2. Peak purity test results obtained from the PDA detector confirmed that the AMB peak was homogeneous and pure in all the analyzed stress samples. Insignificant change in assay of AMB in the presence of related substances and peak purity results of stress samples confirm the specificity and stability-indicating ability of the developed method.

Characterization of AMB and its DPs by LC-MS/MS

AMB and all the DPs (DP-1 to DP-6) were well separated by LC and their retention times (t_R) are given in Table 3. AMB, DP-1, DP-3, DP-5, and DP-6 exhibited abundant protonated molecular ions ($[M + H]^+$) in positive ionization mode whereas DP-2 showed abundant molecular ion ($[M - H]^-$) in negative ionization mode. Collision induced dissociation (CID) spectra of the molecular ions

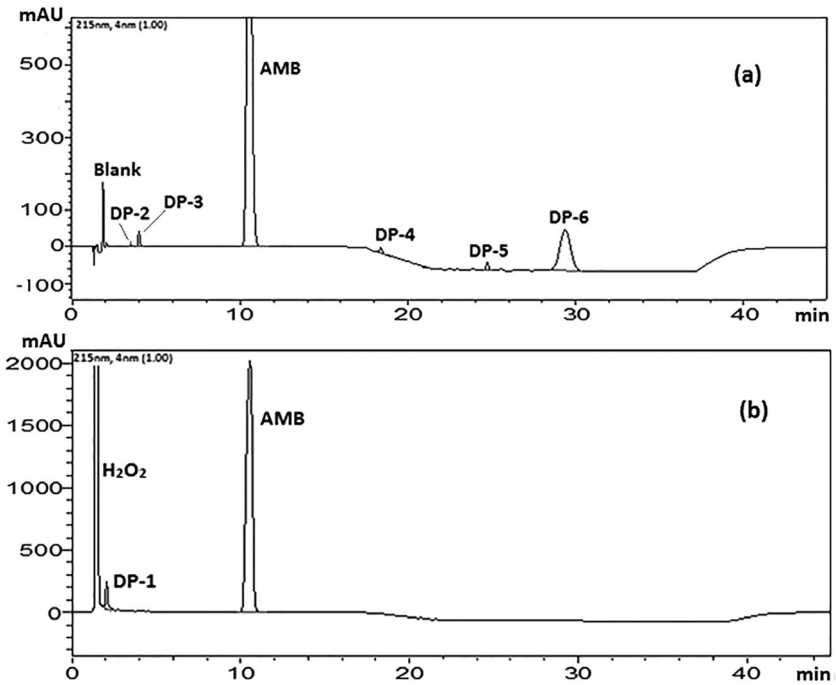

Fig. 2 Chromatograms of AMB: (a) acidic stress and (b) oxidative stress samples.

Table 2 Summary of forced degradation of AMB

Stress conditions	Time	Assay of ambrisentan (% w/w)	Mass balance (assay + total impurities) (% w/w)	Remarks
Acid hydrolysis (0.5 N HCl, 60 °C)	3 h	83.9	99.8	Five degradation products (DP-2, DP-3, DP-4, DP-5, and DP-6) were observed
Base hydrolysis (0.5 N NaOH, 60 °C)	8 h	99.7	99.7	No degradation was observed
Water hydrolysis (60 °C)	8 h	99.2	99.2	No degradation was observed
Oxidation (10% H_2O_2)	24 h	98.2	99.7	One degradation product (DP-1) was observed
Thermal (60 °C)	10 days	99.9	99.9	No degradation was observed
Photo (UV light)	10 days	99.3	99.3	No degradation was observed

of AMB and DPs were recorded to obtain structural information. For CID experiments, the AMB was directly infused into the ESI source and on line LC-ESI-MS/MS experiments were performed to characterize all the DPs formed under various stress conditions. The fragmentation patterns were obtained based on MS/MS experiments and accurate mass measurements from high resolution mass spectral (HRMS) data. The ESI-MS/MS spectra of AMB and all the DPs (except DP-4, no MS/MS achieved) are shown in Fig. 3, and the proposed fragmentation patterns of their molecular ions are shown in Schemes 2 to 7. The elemental composition of molecular ions of AMB and all the DPs and their fragment ions obtained from HRMS data are summarized in Table 3.

MS/MS of AMB (*m*/*z* 379)

To elucidate the degradation behavior of AMB, the ESI-MS spectrum of its abundant protonated molecular ion ($[M + H]^+$) of *m*/*z* 379 was examined. The ESI-MS/MS spectrum of $[M + H]^+$ ion of AMB showed abundant product ions at *m*/*z* 347 and 303 which might be due to 2-carboxy-2-((4,6-dimethylpyrimidin-2-yl)oxy)-1,1-diphenylethan-1-ylium ion (loss of CH_3OH from *m*/*z* 379) and protonated 2-((2,2-diphenylvinyl)oxy)-4,6-dimethylpyrimidine (loss of CH_3OH followed by CO_2 from *m*/*z* 379), respectively. These two product ions confirm the presence of the methoxy and carboxyl groups in AMB molecule. In addition, the spectrum also showed low abundant product ions at *m*/*z* 329 and 125. The ion at *m*/*z* 329 ((2-((4,6-dimethylpyrimidin-2-yl)oxy)-3,3-diphenylallylidyne)oxonium) might be formed due to the loss of CH_3OH followed by loss of a H_2O molecule from *m*/*z* 379, and the ion of *m*/*z* 125 might be due to the formation of protonated 4,6-dimethylpyrimidin-2-ol from *m*/*z* 379, confirming the presence of dimethyl and oxy-group substituted pyrimidine moiety in AMB molecule. The elemental compositions of all these proposed fragment ions (Scheme 2) have been confirmed by accurate mass measurements and are given in Table 3.

Table 3 Elemental compositions of molecular and fragment ions in MS/MS spectra of AMB (*m*/*z* 379), DP-1 (*m*/*z* 395), DP-2 (*m*/*z* 271), DP-3 (*m*/*z* 125), DP-5 (*m*/*z* 183), and DP-6 (*m*/*z* 303)

Analyte (t_R in min)	Proposed formula	Observed mass (Da)	Calculated mass (Da)	Error (ppm)	Proposed neutral loss
Ambrisentan *m*/*z* 379 (10.6)	$C_{22}H_{23}N_2O_4$	379.1652	379.1657	−1.32	
	$C_{21}H_{19}N_2O_3$	347.1386	347.1395	−2.59	CH_3OH
	$C_{21}H_{17}N_2O_2$	329.1287	329.1290	−0.91	CH_3OH, H_2O
	$C_{20}H_{19}N_2O$	303.1488	303.1497	−2.97	CO_2, CH_3OH
	$C_6H_9N_2O$	125.0709	125.0714	−4.00	$C_{16}H_{14}O_3$
DP-1 *m*/*z* 395 (2.1)	$C_{22}H_{23}N_2O_5$	395.1600	395.1606	−1.52	
	$C_{22}H_{21}N_2O_4$	377.1491	377.1501	−2.65	H_2O
	$C_{21}H_{19}N_2O_4$	363.1328	363.1344	−4.41	CH_3OH
	$C_{20}H_{19}N_2O_2$	319.1462	319.1446	5.01	CO_2, CH_3OH
	$C_{16}H_{12}NO_3$	266.0801	266.0817	−6.01	$C_6H_{11}NO_2$
	$C_{16}H_{15}O_3$	255.1024	255.1021	1.18	$C_6H_8N_2O_2$
	$C_{14}H_{11}$	179.0854	179.0860	−3.35	$C_8H_{12}N_2O_5$
	$C_6H_9N_2O_2$	141.0659	141.0664	−3.54	$C_{16}H_{14}O_3$
	$C_8H_9O_2$	137.0602	137.0594	5.84	$C_{14}H_{14}N_2O_3$
	C_7H_5O	105.0336	105.0340	−3.81	$C_{15}H_{18}N_2O_4$
	C_5H_6N	80.0501	80.0500	1.25	CH_3O_2
	$C_2H_7N_2$	59.0615	59.0609	10.16	$C_{20}H_{16}O_5$
DP-2 *m*/*z* 271 (3.5)	$C_{16}H_{15}O_4$	271.0980	271.0976	1.62	
	$C_{14}H_{13}O$	197.0969	197.0972	−1.57	CO_2, CH_2O
	$C_{14}H_{11}O$	195.0812	197.0815	−1.70	CO_2, CH_3OH
	C_8H_7O	119.0493	119.0502	−7.55	C_6H_6
	C_2HO_3	72.9920	72.9931	−14.83	$C_{14}H_{14}O$
DP-3 *m*/*z* 125 (3.9)	$C_6H_9N_2O$	125.0709	125.0714	−4.00	
	$C_6H_7N_2$	107.0605	107.0609	−3.74	H_2O
	C_5H_8N	82.0660	82.0656	4.87	CHNO
	C_5H_6N	80.0500	80.0500	0	CH_3NO
	$C_3H_3N_2$	67.0301	67.0296	7.46	C_3H_6O
	CH_5N_2O	61.0524	61.0527	−4.91	C_5H_4
	C_2H_6NO	60.0453	60.0449	6.66	C_4H_3N
	CH_3N_2	43.0286	43.0296	−23.24	C_5H_6O
	C_2H_4N	42.0340	42.0343	−7.14	C_4H_5NO
	CH_5O	33.0344	33.0340	12.11	C_5H_4O
DP-5 *m*/*z* 183 (24.7)	$C_{13}H_{11}O$	183.0802	183.0804	1.09	
	C_7H_5O	105.0336	105.0335	−0.95	C_6H_6
	C_6H_7O	95.0493	95.0491	−2.10	C_7H_4
	C_6H_5	77.0388	77.0386	−2.60	C_7H_6O
DP-6 *m*/*z* 303 (29.5)	$C_{20}H_{19}N_2O$	303.1492	303.1497	−1.65	
	$C_{14}H_{11}$	179.0854	179.0860	−3.35	$C_6H_8N_2O$
	$C_6H_9N_2O$	125.0709	125.0714	−4.00	$C_{14}H_{10}$

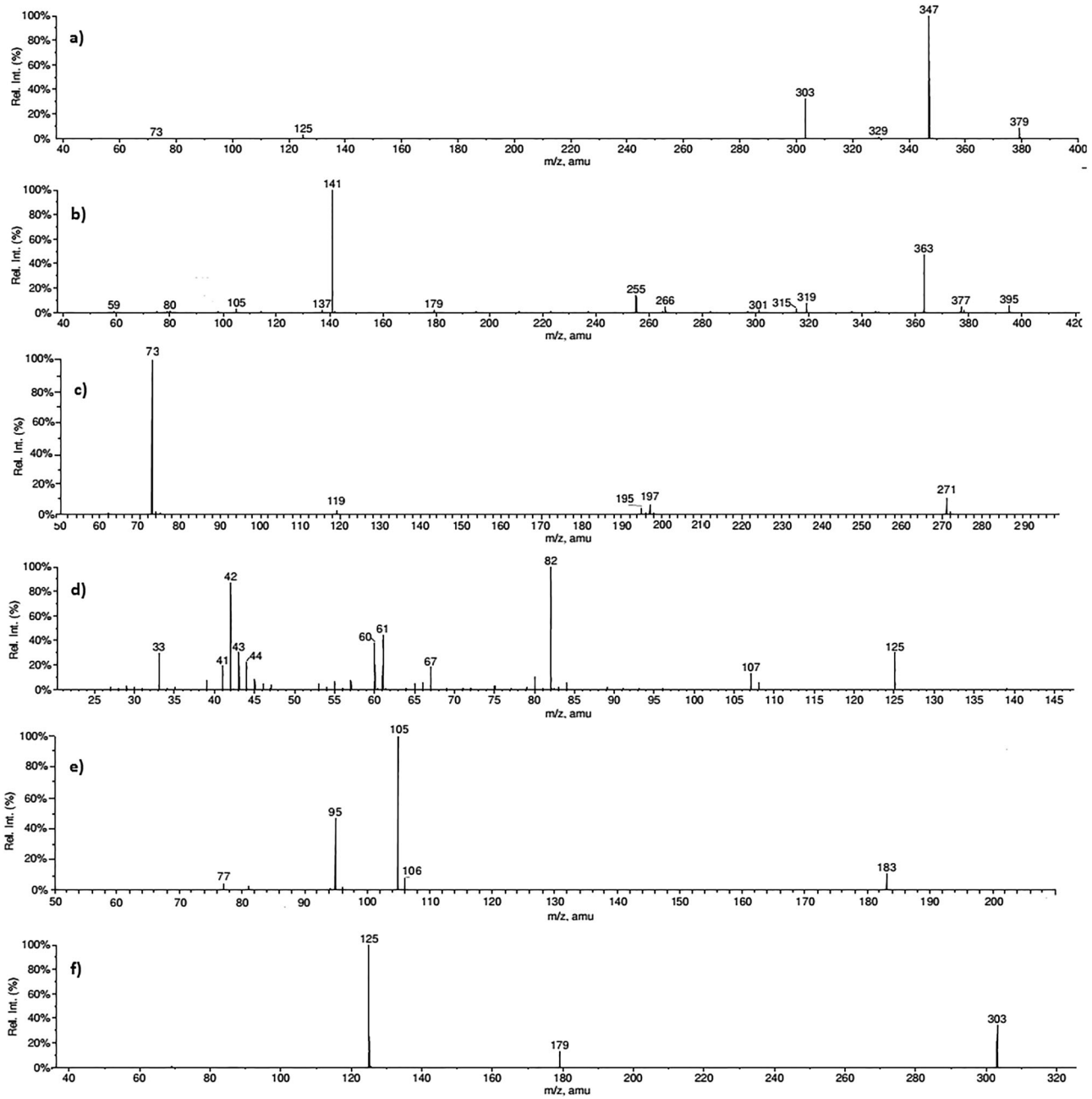

Fig. 3 ESI-MS/MS spectra of molecular ions of (a) AMB, (b) DP-1, (c) DP-2, (d) DP-3, (e) DP-5, and (f) DP-6.

MS/MS of degradation products

DP-1 (*m*/*z* 395). The ESI-MS/MS spectrum of the ion *m*/*z* 395 corresponding to the $[M + H]^+$ of DP-1 formed in oxidative stress is shown in Fig. 3. The ion of *m*/*z* 395 possibly formed due to the addition of an oxygen atom to AMB during oxidation as it possesses 16 Da more in its molecular mass compared to AMB. It is confirmed by MS/MS studies of *m*/*z* 395 ion and comparison with MS/MS study of AMB. The ESI-MS/MS spectrum of *m*/*z* 395 showed abundant product ions at *m*/*z* 141 (base peak) and 363. The formation of the ion at *m*/*z* 141 (increase of *m*/*z* value by 16 Da might be due to addition of oxygen to *m*/*z* 125) clearly suggests the presence of 2-hydroxy-4,6-dimethylpyrimidine 1-oxide (*i.e.*, oxidation of pyrimidine moiety in AMB molecule during oxidation). The spectrum also showed other abundant product ions at *m*/*z* 363 (*m*/*z* 347 + 16 Da, *i.e.*, loss of CH_3OH from *m*/*z* 395) and *m*/*z* 377 (loss of H_2O from *m*/*z* 395) which are characteristic peaks of *N*-oxide product. In addition, the spectrum also showed low abundant product ions at *m*/*z* 319 (loss of CH_3OH followed by CO_2 from *m*/*z* 379), *m*/*z* 255 (loss of pyrimidine moiety from *m*/*z* 395), *m*/*z* 179 (loss of CH_3OH, CO_2 and pyrimidine groups from *m*/*z* 395), *m*/*z* 105 (due to the formation of benzylidyneoxonium ion), *m*/*z* 80 (due to the formation of 2,4-dimethylazet-3-ylium ion) and *m*/*z* 59 (due to the formation of 3-hydroxyoxiran-2-ylium

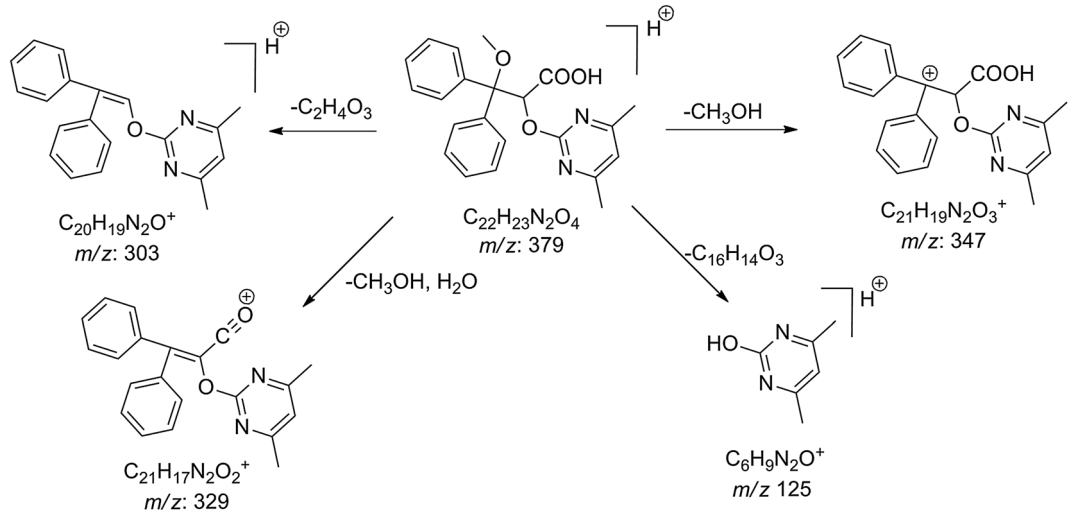

Scheme 2 Proposed fragmentation mechanisms of $[M + H]^+$ ion of AMB.

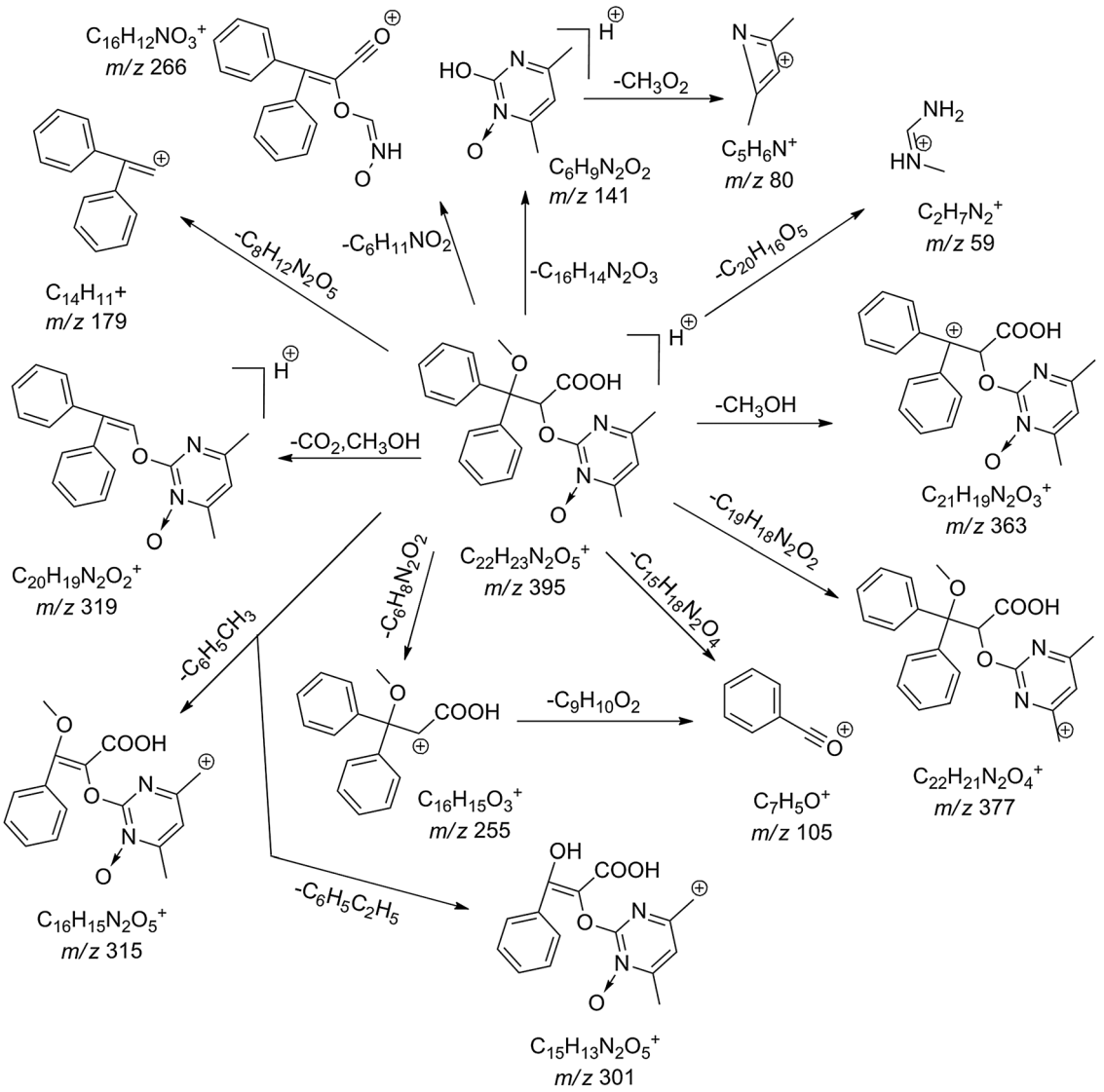

Scheme 3 Proposed fragmentation mechanisms of $[M + H]^+$ ion of DP-1.

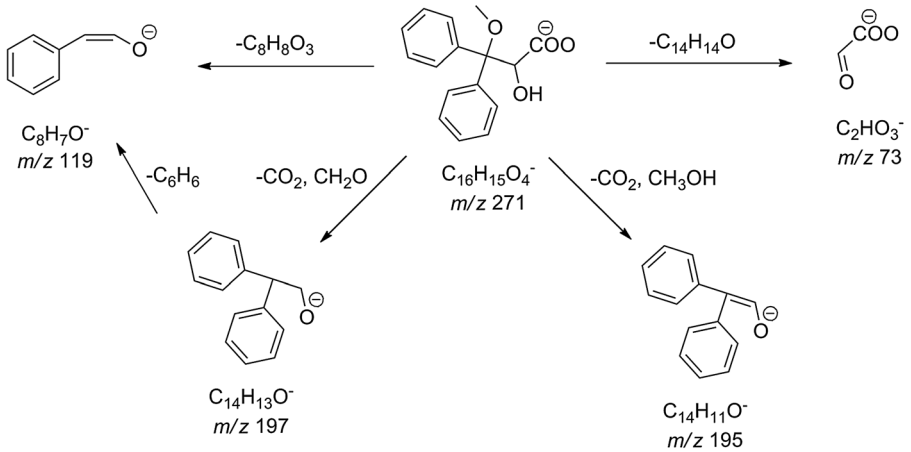

Scheme 4 Proposed fragmentation mechanisms of $[M - H]^-$ ion of DP-2.

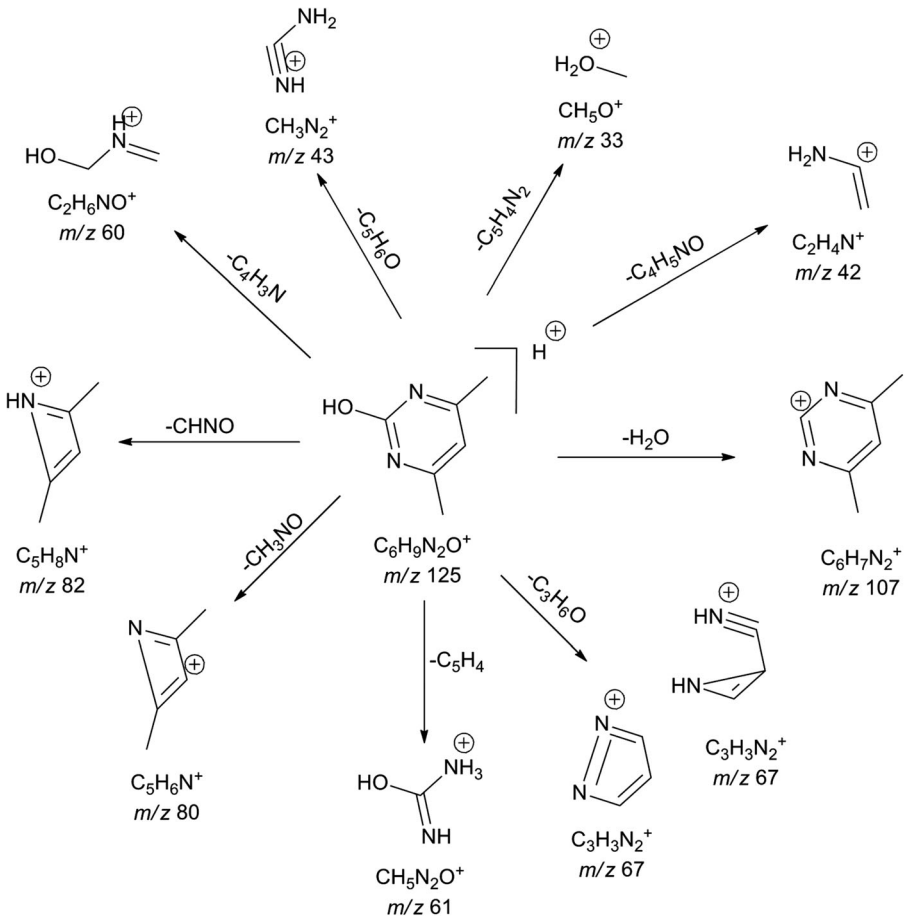

Scheme 5 Proposed fragmentation mechanisms of $[M + H]^+$ ion of DP-3.

ion). The formation of product ions at *m/z* 377, 363, 319, 255, 179, and 141 clearly indicates the presence of an oxygen atom on the pyrimidine moiety in DP-1. The elemental compositions of DP-1 and all its fragment ions (Scheme 3) have been confirmed by accurate mass measurements and are given in Table 3. Therefore, DP-1 was identified as 2-(1-carboxy-2-methoxy-2,2-diphenylethoxy)-4,6-dimethylpyrimidine 1-oxide.

DP-2 (*m/z* 271). The ESI-MS spectrum of the degradation product DP-2 showed an abundant molecular ion at *m/z* 271 ($[M - H]^-$) under negative ionization mode. The ESI-MS/MS spectrum of *m/z* 271 (Fig. 3) showed abundant product ion at *m/z* 73 (base peak) which might be due to 2-oxoacetate formed by the loss of (methoxymethylene)dibenzene. In addition, the spectrum also include low abundant product ions at *m/z* 197,

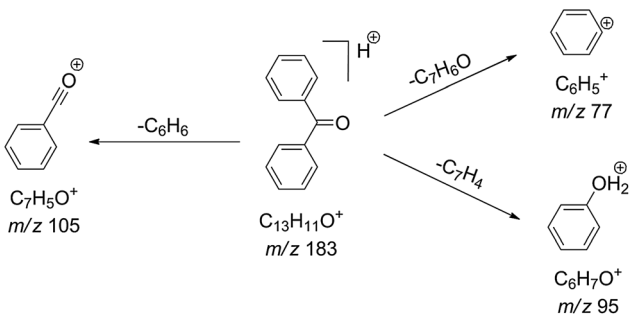

Scheme 6 Proposed fragmentation mechanisms of $[M + H]^+$ ion of DP-5.

195, and 119. The ion at *m/z* 197 may correspond to 2,2-diphenylethanol anion formed by the loss of CO_2 followed by CH_2O from $[M - H]^-$ ion, the ion at *m/z* 195 may correspond to 2,2-diphenylethenol anion formed by the loss of CO_2 followed by CH_3OH from $[M - H]^-$ ion, and the ion at 119 may correspond to 2-phenylethenol anion formed by the loss of $C_8H_8O_3$ from $[M - H]^-$ ion or C_6H_6 from *m/z* 197. All these product ions confirm the presence of two phenyl and carboxylic acid groups in the molecular structure of DP-2. Moreover, its retention time and molecular masses were matched with Imp-4. Peak purity test and CID experimental studies of Imp-4 confirm it as one of the degradation products DP-2. The elemental compositions of molecular ion ($[M - H]^-$) of DP-2 and all its fragmentation ions have been confirmed by accurate mass measurements and are shown in Table 3. From the above discussion on the fragmentation pattern (Scheme 4), DP-2 was identified as 2-hydroxy-3-methoxy-3,3-diphenylpropanoic acid.

DP-3 (*m/z* 125). The ESI-MS/MS spectrum of the ion *m/z* 125 corresponding to the $[M + H]^+$ of DP-3 formed in acidic stress is shown in Fig. 3, and it showed abundant product ions at *m/z* 82, 61, 60, and 42. The product ion at *m/z* 82 (2,4-dimethylazet-1-ium ion) might be resulted by the loss of cyanic acid from *m/z* 125. The ions at *m/z* 61 (isouronium ion), *m/z* 60 (1-hydroxy-*N*-methylenemethanaminium ion), and *m/z* 42 (etheniminium ion) might result due to loss of C_5H_4, C_4H_3N, and C_4H_5NO from *m/z* 125, respectively. In addition, the spectrum also showed low abundance product ions at *m/z* 107 (loss of H_2O from *m/z* 125), *m/z* 80 (loss of formimidic acid from *m/z* 125), *m/z* 67 (((1*H*-azirin-2-yl)methylidyne)ammonium), *m/z* 43 (protonated cyanamide), and *m/z* 33 (methyloxonium ion). The formation of ions at *m/z* 107, 61, and 33 indicates the presence of pyrimidine moiety, urea type functional group linkage and –C–OH group, respectively, in the molecular structure of *m/z* 125. The elemental compositions of all these ions have been confirmed by accurate mass measurements and are given in Table 3. From the above fragmentation pattern (Scheme 5), DP-3 was identified as 4,6-dimethylpyrimidin-2-ol.

DP-4 (*m/z* 319). The ESI-MS spectrum of the minor degradation product DP-4 showed a low intensity molecular ion peak at *m/z* 319. The fragmentation in CID experiments was not successful because of low abundance molecular ion peak. Hence a possible structure of DP-4 could not be proposed.

DP-5 (*m/z* 183). The ESI-MS/MS spectrum $[M + H]^+$ ion of the minor degradation product DP-5 (*m/z* 183) formed in acidic stress is shown in Fig. 3, and it showed two abundant product ions at *m/z* 105 (base peak) and 95. The product ion at *m/z* 105 show a decrease in mass by 78 Da compared to *m/z* 183, and may be formed by the loss of C_6H_6 from *m/z* 183 resulting in a benzylidyneoxonium ion. The ion at *m/z* 95 may be formed due to formation of protonated phenol. In addition, the spectrum also showed a low abundant product ion at *m/z* 77 which may be due phenyl ion by loss of C_6H_5CHO (−106 Da) from *m/z* 183. The formation of ions at *m/z* 105 and 77 confirms the presence of two phenyl rings with a carbonyl substitution in the molecular structure of DP-5, *i.e.*, the ion at *m/z* 183 (DP-5) may be due to protonated benzophenone which is one of the process related impurities (Imp-1) of ambrisentan. The elemental compositions of molecular ion ($[M + H]^+$) of DP-5 and all its fragmentation ions (Scheme 6) have been confirmed by accurate mass measurements and are shown in Table 3. The formation of DP-5 (benzophenone) during stress is also checked by comparing the fragmentation pattern obtained for Imp-1. The obtained similar patterns for both Imp-1 and DP-5 confirm DP-5 as benzophenone.

DP-6 (*m/z* 303). The ESI-MS/MS spectrum of the ion *m/z* 303 corresponding to the $[M + H]^+$ of major degradation product DP-6 formed in acidic stress is shown in Fig. 3. The MS/MS spectrum of *m/z* 303 showed only two abundant product ions at *m/z* 179 and 125. Unlike the ambrisentan (*m/z* 379) spectrum, the product ion spectrum of DP-6 (*m/z* 303) showed no product ions corresponding to the loss of CH_3OH (−32 Da) and CO_2 (−44 Da), clearly indicating the absence of methoxy and carboxylic acid groups in its molecular structure. Exact loss of mass by 76 Da (32 + 44) clearly matches with the *m/z* value of DP-6. This may result of the C=C double bond between diphenyl and pyrimidine moieties in its molecular structure. It is confirmed by its product ion spectrum. The base peak at

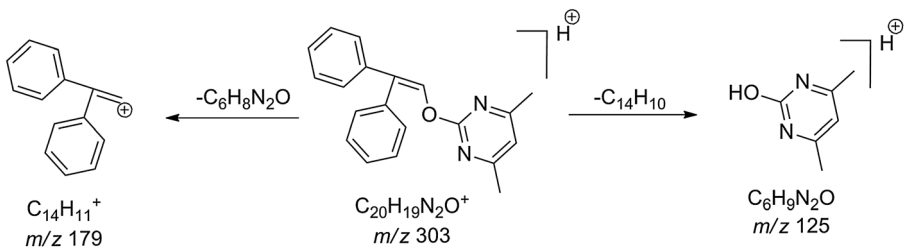

Scheme 7 Proposed fragmentation mechanisms of $[M + H]^+$ ion of DP-6.

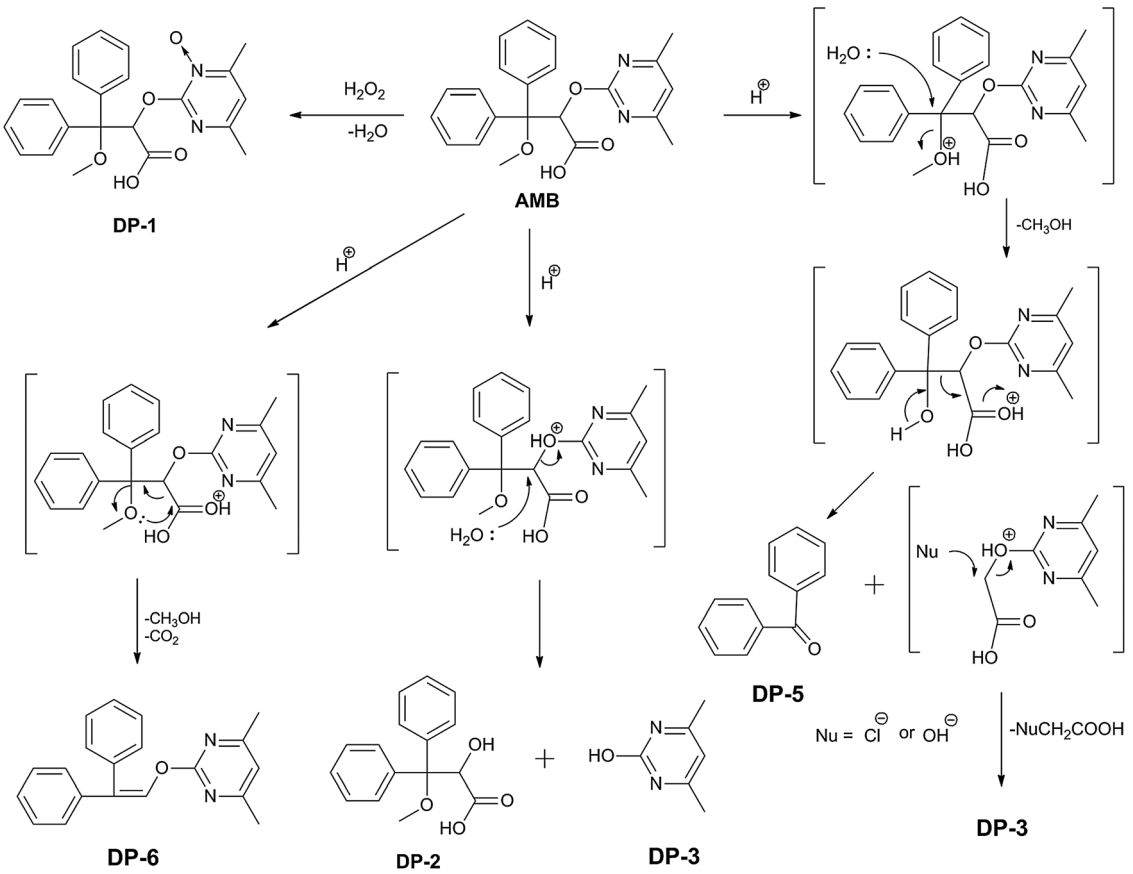

Scheme 8 Mechanism of degradation of AMB in acidic and oxidative stress conditions.

m/*z* 125 might be due to the formation of 4,6-dimethylpyrimidin-2-ol by the loss of a biphenyl substituted ethylene moiety (*i.e.*, ethene-1,1-diyldibenzene, −178 Da) attached to the pyrimidine ring. The product ion at *m*/*z* 179 might be formed due to the formation of 2,2-diphenylethen-1-ylium ion by the loss of a pyrimidine moiety (−124 Da) from *m*/*z* 303. From these fragmentation studies (Scheme 7), DP-6 was identified as 2-((2,2-diphenylvinyl)oxy)-4,6-dimethylpyrimidine. The elemental compositions DP-6 and its fragment ions have been confirmed by accurate mass measurements and are given in Table 3.

Mechanism of degradation

The mechanism of formation of degradation products ($DP_{1–3}$ and $DP_{5–6}$) under both acidic and oxidative stress conditions has been proposed. DP-1 in oxidative stress could be formed by the addition of one oxygen atom from H_2O_2 to one of the nitrogens of the pyrimidine moiety of ambrisentan. DP-2 and DP-3 might be due to the hydrolytic cleavage of C–O bond present between pyrimidine and diphenyl moieties in ambrisentan in an acidic medium. The formation of DP-5 is relatively complex and it could be due to the hydrolysis of methoxy group followed by the loss of the pyrimidine moiety, whereas DP-6 could be formed by the loss of methoxy and CO_2 groups present in ambrisentan. A pictorial representation of mechanism of formation of DPs is shown in Scheme 8.

Conclusions

The degradation behavior of ambrisentan was studied under various stress conditions as per International Conference on Harmonization (ICH) prescribed guidelines. In total, six degradation products were formed and five of them were characterized by liquid chromatography and tandem mass spectrometry and accurate mass measurements. A simple gradient reversed phase high performance liquid chromatographic method has been developed and validated for the determination of a stability-indicating assay of ambrisentan and its five related substances in bulk drugs. The developed method has been found to be selective, precise, linear, accurate, and sensitive, and is applicable for detecting process related impurities and other possible degradation products which may be present at trace levels in bulk drugs. Thus, the method can be used for process development as well as quality assurance of ambrisentan in bulk drugs.

Acknowledgements

The authors thank Director, IICT, Hyderabad, India for encouragement and permission to communicate results for publication. RK thanks CSIR, New Delhi, for a Research Fellowship.

References

1 J. D. Croxtall and S. J. Keam, *Drugs*, 2008, **68**, 2195.
2 H. W. Farber and J. Loscalzo, *N. Engl. J. Med.*, 2004, **351**, 1655.
3 J. R. Klinger, R. J. Oudiz, R. Spence, D. Despain and C. Dufton, *Am. J. Cardiol.*, 2011, **108**, 302.
4 N. Galiè, D. Badesch, R. Oudiz, G. Simonneau, M. D. McGoon, A. M. Keogh, A. E. Frost, D. Zwicke, R. Naeije, S. Shapiro, H. Olschewski and L. J. Rubin, *J. Am. Coll. Cardiol.*, 2005, **46**, 529.
5 R. Nirogi, V. Kandikere, P. Komarneni, R. Aleti, N. S. P. Padala and I. Kalaikadhiban, *Biomed. Chromatogr.*, 2012, **26**, 1150.
6 R. K. Kaja, K. V. SurendhraNath, K. Babuji, P. V. V. Satyanarayana and K. S. Kumar, *Anal. Chem.: Indian J.*, 2009, **8**, 155.
7 M. Douŝa and P. Gibala, *J. Sep. Sci.*, 2012, **35**, 798.
8 N. Satheeshkumar and G. Naveenkumar, *J. Chromatogr. Sci.*, 2013, DOI: 10.1093/chromsci/bmt138.
9 M. B. V. Narayana, K. B. Chandrasekhar and B. M. Rao, *J. Chromatogr. Sci.*, 2013, DOI: 10.1093/chromsci/bmt121.
10 H. Riechers, H. P. Albrecht, W. Amberg, E. Baumann, H. Bernard, H. J. Böhm, D. Klinge, A. Kling, S. Müller, M. Raschack, L. Unger, N. Walker and W. Wernet, *J. Med. Chem.*, 1996, **39**, 2123.
11 L. A. Sorbera and J. Castaner, *Drugs Future*, 2005, **30**, 765.
12 ICH. 2003. Q1A(R2): Stability testing of new drug substances and products.
13 ICH. 2003. Q2(R1): Validation of analytical procedures: test and methodology.